

MSM-Metal Semiconductor Metal Photo-detector Using Black Silicon Germanium (SiGe) for Extended Wavelength Near Infrared Detection

**by Fred Semendy, Patrick Taylor, Gregory Meissner,
and Priyalal Wijewarnasuriya**

ARL-TR-6176

September 2012

NOTICES

Disclaimers

The findings in this report are not to be construed as an official Department of the Army position unless so designated by other authorized documents.

Citation of manufacturer's or trade names does not constitute an official endorsement or approval of the use thereof.

Destroy this report when it is no longer needed. Do not return it to the originator.

Army Research Laboratory

Adelphi, MD 20783-1197

ARL-TR-6176**September 2012**

MSM-Metal Semiconductor Metal Photo-detector Using Black Silicon Germanium (SiGe) for Extended Wavelength Near Infrared Detection

**Fred Semendy, Patrick Taylor, Gregory Meissner,
and Priyalal Wijewarnasuriya
Sensors and Electron Devices Directorate, ARL**

REPORT DOCUMENTATION PAGE				Form Approved OMB No. 0704-0188	
<p>Public reporting burden for this collection of information is estimated to average 1 hour per response, including the time for reviewing instructions, searching existing data sources, gathering and maintaining the data needed, and completing and reviewing the collection information. Send comments regarding this burden estimate or any other aspect of this collection of information, including suggestions for reducing the burden, to Department of Defense, Washington Headquarters Services, Directorate for Information Operations and Reports (0704-0188), 1215 Jefferson Davis Highway, Suite 1204, Arlington, VA 22202-4302. Respondents should be aware that notwithstanding any other provision of law, no person shall be subject to any penalty for failing to comply with a collection of information if it does not display a currently valid OMB control number.</p> <p>PLEASE DO NOT RETURN YOUR FORM TO THE ABOVE ADDRESS.</p>					
1. REPORT DATE (DD-MM-YYYY)		2. REPORT TYPE		3. DATES COVERED (From - To)	
September 2012					
4. TITLE AND SUBTITLE MSM-Metal Semiconductor Metal Photo-detector Using Black Silicon Germanium (SiGe) for Extended Wavelength Near Infrared Detection				5a. CONTRACT NUMBER	
				5b. GRANT NUMBER	
				5c. PROGRAM ELEMENT NUMBER	
6. AUTHOR(S) Fred Semendy, Patrick Taylor, Gregory Meissner, and Priyalal Wijewarnasuriya				5d. PROJECT NUMBER	
				5e. TASK NUMBER	
				5f. WORK UNIT NUMBER	
7. PERFORMING ORGANIZATION NAME(S) AND ADDRESS(ES) U.S. Army Research Laboratory ATTN: RDRL-SEE-I 2800 Powder Mill Road Adelphi, MD 20783-1197				8. PERFORMING ORGANIZATION REPORT NUMBER ARL-TR-6176	
9. SPONSORING/MONITORING AGENCY NAME(S) AND ADDRESS(ES)				10. SPONSOR/MONITOR'S ACRONYM(S)	
				11. SPONSOR/MONITOR'S REPORT NUMBER(S)	
12. DISTRIBUTION/AVAILABILITY STATEMENT Approved for public release; distribution unlimited.					
13. SUPPLEMENTARY NOTES					
14. ABSTRACT We have investigated for the first time the electrical properties of metal-semiconductor-metal (MSM) photodectors fabricated using black silicon-germanium on silicon substrate ($\text{Si}_{1-x}\text{Ge}_x/\text{Si}$) for I-V, optical response, external quantum efficiency (EQE), internal quantum efficiency (IQE), and responsivity and reflectivity. Silicon-germanium ($\text{Si}_{1-x}\text{Ge}_x$)/Si with variations of Ge were blackened by metal enhanced chemical etching (MECE) using nanometer-scale gold particles as catalyst and $\text{HF}:\text{H}_2\text{O}_2:\text{CH}_3\text{COOH}$ solution as etchant. The etched surface was black, textured, and showed strong suppression of reflectivity. These properties are consistent with $\text{Si}_{1-x}\text{Ge}_x$ becoming highly micro-structured due to metal catalysis and wet etching. Using the blackened SiGe/Si, MSM photodiodes were fabricated and tested. The lowering of reflection using a U.S. Army Research Laboratory (ARL)-developed technique has helped the enhancement of absorption in $\text{Si}_{1-x}\text{Ge}_x$ to provide increased optical response, which is an important milestone towards practical, extended wavelength ($\sim 2 \mu\text{m}$) electro-optical applications.					
15. SUBJECT TERMS MSM, SoGe, Detector, MELE, QE, IR application					
16. SECURITY CLASSIFICATION OF:			17. LIMITATION OF ABSTRACT	18. NUMBER OF PAGES	19a. NAME OF RESPONSIBLE PERSON
a. REPORT	b. ABSTRACT	c. THIS PAGE			Fred Semendy
UNCLASSIFIED	UNCLASSIFIED	UNCLASSIFIED	UU	18	19b. TELEPHONE NUMBER (Include area code) (301) 394-4627

Contents

List of Figures	iv
1. Introduction	1
2. Experimental Details	3
3. Result and Discussion	6
4. Conclusion	8
5. References	9
Distribution List	11

List of Figures

Figure 1. Basic structure of MSM photo detector (a) $\text{Si}_{1-x}\text{Ge}_x/\text{Si}$ material and (b) MSM device.	3
Figure 2. Block diagram of IQE 200 EQE/IQE measurement system.	5
Figure 3. Depiction of the beam splitter and its effect on the optical beam.	5
Figure 4. I-V curves for $\text{Si}_{1-x}\text{Ge}_x/\text{Si}$ MSM photodiodes. (a) 15% Ge with and without 5 mW light (red) and (b) 30% Ge MSM device with 5 (green) and 10 mW lights (Lavender).	6
Figure 5. I-V curves for $\text{Si}_{1-x}\text{Ge}_x/\text{Si}$ MSM photodiodes. (a) 5 min etched 15% Ge with 5 mW light (red) and (b) 15% Ge MSM device with 10 min etch 5 mW illumination.	7
Figure 6. Time based optical response of $\text{Si}_{1-x}\text{Ge}_x/\text{Si}$ MSM detector. (a) response with a GaAs filter, and a Si filter. And (b) with Si filter and varying applied voltage, 0.5 V, 1.0 V, and 1.5 V.	7
Figure 7. (a) Reflectance of the sample $\text{Si}_{0.85}\text{Ge}_{0.15}/\text{Si}$ etched for 10 min (b) QE (λ) and (c) spectral responsivity of the same sample with zero bias	8

1. Introduction

The growth of high quality nano-scaled silicon germanium (SiGe/Si) layers and Ge islands on Si substrates by ultra high vacuum/chemical vapor deposition (UHV/CVD) has attracted intense interest because of the prospect of band gap engineering (1). For large scale infrared (IR) detector systems, SiGe/Si is a favorable material system because of perfect thermal matching to the Si readout circuit and adaptable peak and cut-off wavelength. Some of the important applications of SiGe/Si are satellite imaging and observation, heat sensing, medical diagnostics, and missile tracking. The Army would like to use the SiGe/Si material system as a replacement for an expensive InGaAs detection and imaging system. To make SiGe/Si comparable in efficiency, the reflective property of the material must be reduced and the absorption property has to be increased by using one of the available techniques.

Over the past 10 years, new phenomena based on nanostructuring the surface of Si have been investigated for application to infrared imaging. In 2003, Mazur and colleagues reported that using femtosecond laser processing coupled with halogenated etching gas could produce silicon surfaces having sub-micrometer corrugated conical tip microstructures (1). These microstructures had the special property such that the surface of the silicon was rendered almost perfectly non-reflective. They named this material “black silicon.” In that early study, they showed that when they produced that microstructure using only halogenated etching gas (sulfur hexafluoride [SF₆]), the spectral absorbance of light was extended well beyond that which would be expected from the conventional band-theory understanding of silicon. In subsequent reports from researchers in the Mazur group, evidence began to point to the very highly doped surface region (sulfur-doped) on the etched surface that seemed to promote sub-bandgap absorption (2). In that work, they demonstrated this important result: after forming the etched surface, the extended wavelength infrared absorbance could be decreased and almost completely eliminated because of dopant evaporation during high-temperature annealing. Based on these early results, the Mazur Group partnered with device researchers at the University of Virginia and the University of Texas at Austin to demonstrate a novel infrared detector based on this new material (3).

The researchers in this partnership showed two very important demonstrations: (1) the spectral responsivity was enhanced compared to that of conventional silicon photodetectors, and (2) responsivity was extended to longer infrared wavelengths (1.3 and 1.55 μm), beyond the spectral range generally expected from silicon, which is limited to about 1.1 μm . While there is some uncertainty about the mechanism that enables sub-bandgap, longer wavelength detection, the mechanism is currently explained as longer wavelength photons excite carriers across the energy difference between mid-gap defect states from the heavily doped region and the

conduction band edge. While the science behind the phenomena is being resolved, these interesting results presage new, low-cost near-infrared detectors that could have important military and civilian applications. However, for tactical military applications, a much higher spectral response at extended wavelengths in the near-infrared ($\sim 2 \mu\text{m}$) would be desired. To that end, we are investigating $\text{Si}_{1-x}\text{Ge}_x$ materials with the goal of obtaining an improved photo response out to $2 \mu\text{m}$ by (1) shrinking the bandgap so that the *difference between the conduction band-edge and the defect state is reduced* and (2) providing a naturally larger absorption coefficient for longer wavelength light. So this work builds upon the results reported from the Mazur and partner groups, and investigates new heavily doped black $\text{Si}_{1-x}\text{Ge}_x$ materials. Some important differences between this work and the approach of the Mazur and partner groups are (1) we employ a metal-masked, wet-chemical etching approach versus a femtosecond gas-phase etching process, and (2) we used in-situ boron doping $p \approx 5 \times 10^{19}/\text{cm}^3$ versus sulfur doping $n \approx 5 \times 10^{20}/\text{cm}^3$ from the past work.

Our investigation with black $\text{Si}_{1-x}\text{Ge}_x$ is very important since SiGe is a good substitute material for Si for many applications in low-power and high-speed semiconductor device technologies (4, 5). It is a promising material for quantum well devices (6), infrared detectors (7), and modulation doped field-effect transistors (MODFET) (8, 9). Recently, much work has been planned to use $\text{Si}_{1-x}\text{Ge}_x$ for optodetectors and micro-electro-mechanical systems (MEMS) sensors and actuators. Activity is also being continued to develop flip chip optical receivers. Among the many other applications currently being considered are strained SiGe on silicon to be used as base in a heterojunction bipolar transistor (HBT) in a bipolar complementary metal oxide semiconductor (BiCMOS) process and complementary metal oxide semiconductor (CMOS) logic applications. SiGe has much to offer for the fabrication of devices with improved efficiency (10). In a particular instance, self-assembled Ge-islands and black Ge based on nano-needle arrays have been developed (11). Increased absorption of light is essential to create highly efficient opto-sensors and photovoltaic devices. To achieve this, efficient three-dimensional (3-D) structures with relevant material systems are required. Apart from these two techniques, others (12, 13) have proposed a technique in which multicrystalline SiGe bulk crystal with microscopic compositional distribution is grown using the casting technique. The average Ge composition was changed systematically between 0% and 10%. A small addition of Ge to multicrystalline Si was found to be very effective to increase the short-circuit current density without affecting open circuit voltage. They also indicated that such grown SiGe materials are promising candidates for solar cell and other opto-electronic applications. For such applications, SiGe has to be prepared with reduced reflectivity and increased absorbance. This can be achieved through surface texturing, as has been used in the case of black silicon. In general, for a 3-D blackened surface, reactive ion etching or wet anisotropic etching are the techniques of choice. Although reactive ion etching can provide a structure with a high aspect ratio, it involves rather complicated procedures. Metal enhanced chemical etching (MECE) (14, 15), by which silicon is etched using

metal thin films or particle as catalysts, is an attractive procedure because it is simple and easier to perform with good results.

SiGe/Si heterostructures are expected to play a major role in Si-based optoelectronics (16, 17). Recent advances in SiGe heteroepitaxy techniques for the growth of strained $\text{Si}_{1-x}\text{Ge}_x$ layers have extended their applications in Si-optoelectronics. The importance of Si/SiGe strained layers lies in the possibility of integrating optoelectronic devices. Due to the compressive strain in SiGe alloy films, the bandgap of $\text{Si}_{1-x}\text{Ge}_x$ alloys can be tailored continuously from Si ($x=0$, 1.17 eV) to Ge (for $x=1$, 0.66 eV) at room temperature (18). Si is transparent in the 1.3–1.6 μm wavelength range, and the SiGe absorption edge shifts towards the red with increasing Ge fraction. The shift offers a means absorbing 1.3–1.6 μm light, if desired by choosing $x > 0.3$ for 1.3 μm light and $x > 0.85$ μm for 1.55 μm .

2. Experimental Details

The $\text{Si}_{(x)}\text{Ge}_{(1-x)}$ alloy layers in this work were grown on 8-in silicon substrates having either (111) or (100) orientation and etched as described in (19). Etched $\text{Si}_{1-x}\text{Ge}_x/\text{Si}$ with varying Ge concentration was used for the fabrication of the metal semiconductor metal (MSM) photodetector. Standard processing techniques were used. After defining the pattern on the top surface, Schottky metal contacts were made on the surface of the absorption layer. Here the device is in contrast to the normal Schottky photodiode that has top and bottom metal contacts. The MSM pattern has two back-to-back diodes in series—one forward-biased and the other reverse-biased. In the dark condition, there is only a little reverse saturation current produced in the biased photodetector, which is called the dark current of the device. Figure 1 depicts the structure of the MSM.

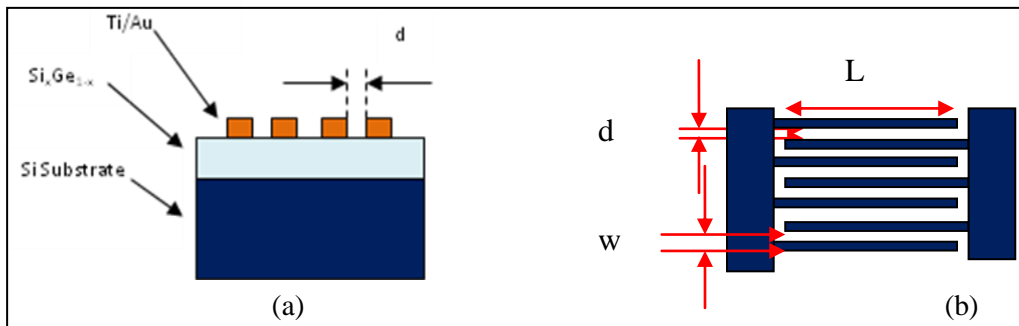


Figure 1. Basic structure of MSM photo detector (a) $\text{Si}_{1-x}\text{Ge}_x/\text{Si}$ material and (b) MSM device.

When light is shone onto the surface of the device, it will be absorbed within the underlying semiconductor at a depth depending upon the wavelength and the absorption coefficient of the

material. It is worth mentioning here that we have modified the semiconductor surface with the intention of increasing the absorption, thus increasing the quantum efficiency and responsivity. The absorbed light will produce electron-hole pairs, and with an application of a bias to the metal fingers, an electric field will be created within the underlying semiconductor that sweeps the photo-generated carrier out of the depletion region resulting in a photocurrent. The collection efficiency of the MSM will depend upon the magnitude of the applied voltage and finger separation (d). The metal fingers are fabricated with Ti/Au (200 nm/2500 nm). Fabricated devices were used for I-V measurements using Agilent 4160 Parametric Analyzer to obtain the dark current, as well as optical response under varying optical power. A broadband source was used for the input light.

We used the Oriel IQE-200 EQE/IQE measurement for extended wavelength range to measure the QE. The IQE 200 incorporates a novel geometry that splits the beam, allowing for simultaneous measurement of EQE (external quantum efficiency) and the reflective losses to quantify IQE (internal quantum efficiency). The power spectral responsivity $R_{pa}(\lambda)$ for collected electrons per incident photons may be converted to external quantum efficiency QE (λ), and then to IQE (λ), using the equations,

$$QE(\lambda) = \frac{hc}{q} \frac{R_{pa}(\lambda)}{\lambda} \quad (1)$$

$$IQE(\lambda) = \frac{QE(\lambda)}{1 - R_{sample}(\lambda)}, \quad (2)$$

where $R_{sample}(\lambda)$ is effective sample reflectance.

The optical layout of the beam splitter in the IQE 200 system is illustrated in figure 2. It is comprised of one spectrally neutral 50-50 beam splitter and four lenses. The output light from the monochromator is first collimated by lens 1. The collimated light is then split into two beams of which one passes through the beam splitter and is focused by lens 2 onto the Reference Detector. This detector measures the output light of any given wavelength. The other beam is reflected by the beam splitter down onto the sample surface through focusing lens 3 for the QE measurement. The spot size on the sample is determined by the lens 3. Therefore, by varying the lens 3 optical parameters, a variety of spot size options can be obtained. For the internal quantum efficiency measurement, the reflected light from the sample is collimated lens 3 and then a known factor of it passes through the beam splitter. The beam is then focused by lens 4 on to the reflectance detector (figure 3).

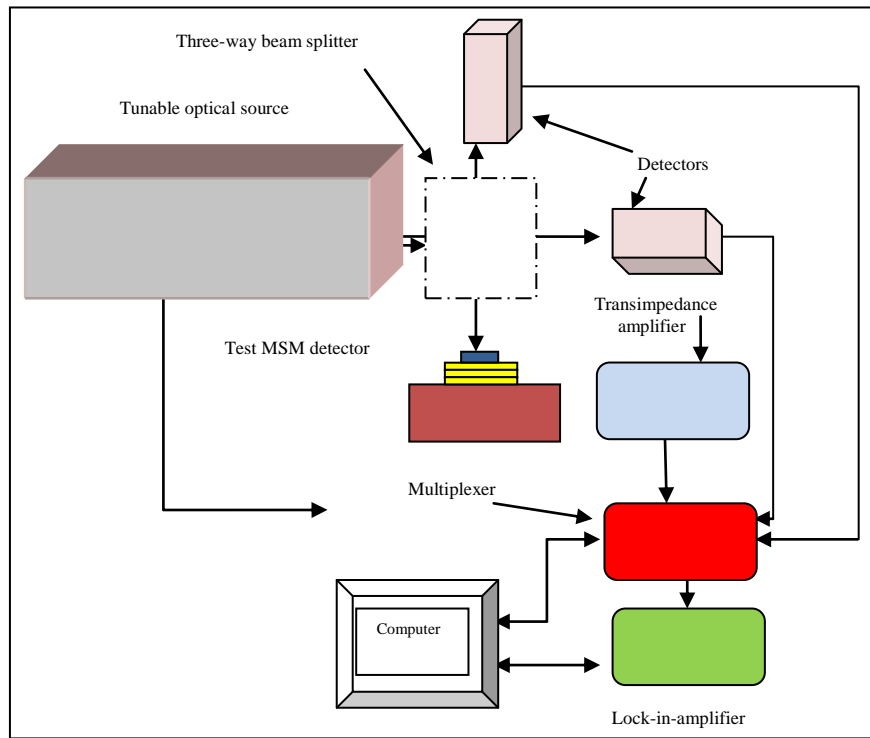


Figure 2. Block diagram of IQE 200 EQE/IQE measurement system.

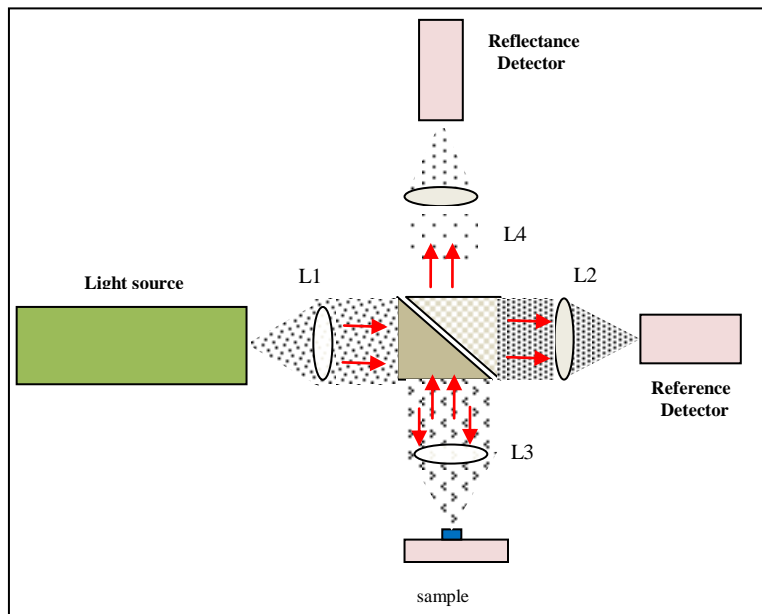


Figure 3. Depiction of the beam splitter and its effect on the optical beam.

3. Result and Discussion

Figures 4a and b give the current-voltage curves of the $\text{Si}_{1-x}\text{Ge}_x/\text{Si}$ MSM detectors, with 15% and 30% Ge-containing samples. The optical illumination was provided by 5 and 10 mW white light sources.

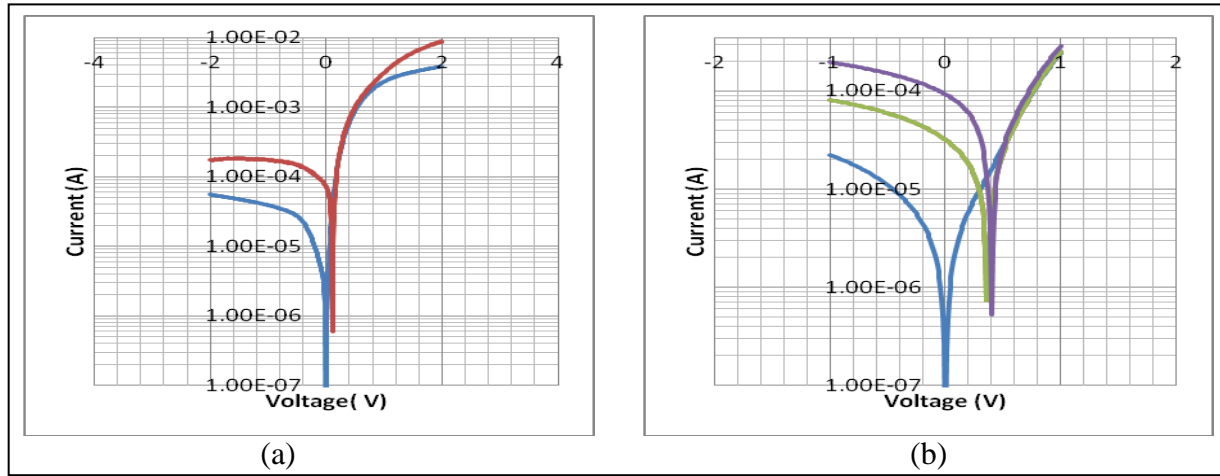


Figure 4. I-V curves for $\text{Si}_{1-x}\text{Ge}_x/\text{Si}$ MSM photodiodes. (a) 15% Ge with and without 5 mW light (red) and (b) 30% Ge MSM device with 5 (green) and 10 mW lights (Lavender).

The clear dependence of the response on the optical power of the illumination source is evident here. The dependence is increased with respect to the amount of Ge in the semiconductor surface.

Figure 5 gives the I-V curves of $\text{Si}_{1-x}\text{Ge}_x/\text{Si}$ with 15% but etched for (a) 5 min and (b) 10 min, followed by the fabrication of MSM detectors. Comparing the results, one can see that there is increased optical response for two similar samples containing the same amount of Ge but with the surface etched for varying times. Clearly, one can observe the enhanced optical response due to greater absorbance of photons on the second sample.

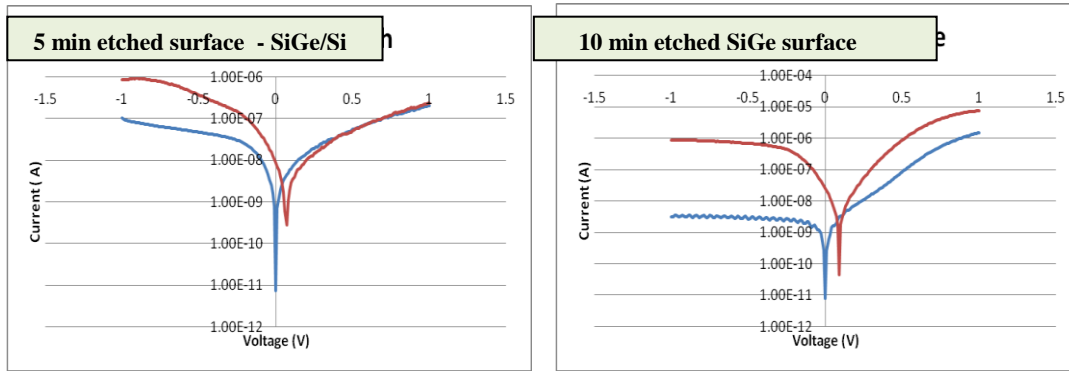


Figure 5. I-V curves for $\text{Si}_{1-x}\text{Ge}_x/\text{Si}$ MSM photodiodes. (a) 5 min etched 15% Ge with 5 mW light (red) and (b) 15% Ge MSM device with 10 min etch 5 mW illumination.

The effect of optical filtering on the optical response was studied in another set of samples, since $\text{Si}_{1-x}\text{Ge}_x/\text{Si}$ is expected to show detection ~ 1600 nm. However, we wanted to see the effect of using a GaAs wafer and a Si wafer as filters. For a particular optical power, current measurements were obtained first for a GaAs filter and then Si filter. In another case for a particular optical power of optical illumination, the time response was recorded for varying voltages. These two cases are shown in figures 6a and b.

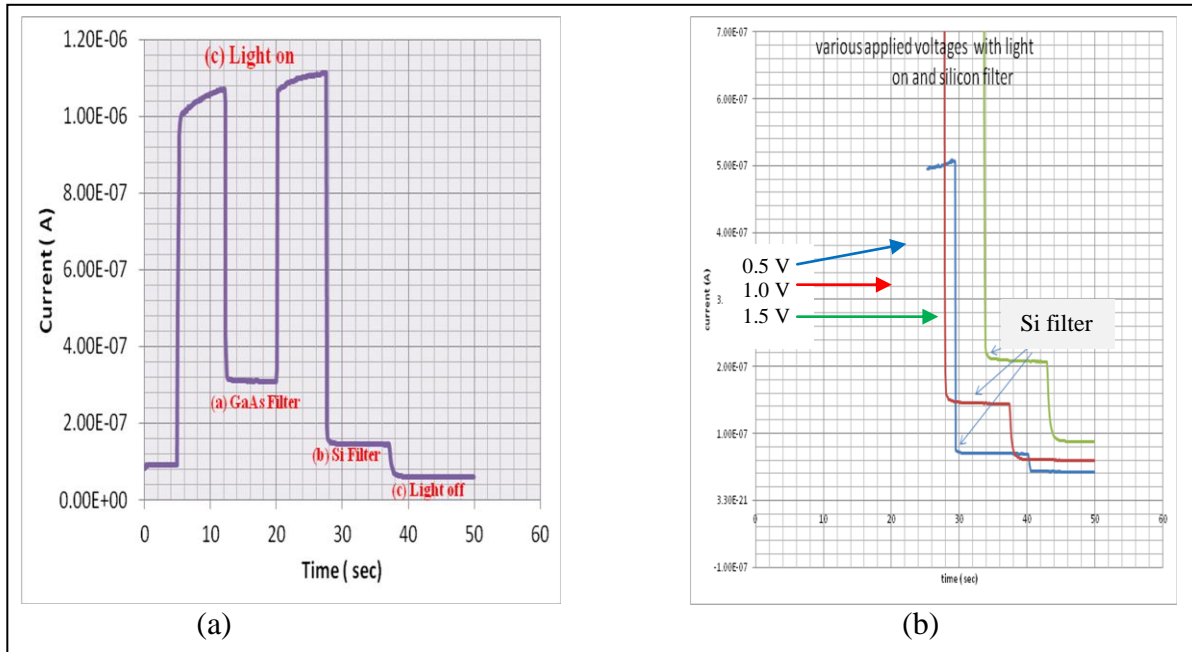


Figure 6. Time based optical response of $\text{Si}_{1-x}\text{Ge}_x/\text{Si}$ MSM detector. (a) response with a GaAs filter, and a Si filter. (b) with Si filter and varying applied voltage, 0.5 V, 1.0 V, and 1.5 V.

Using GaAs filter has shown the effect of filtered optical beam beyond 960 nm, and the amplitude of the response current has dropped substantially to about 70% of the unfiltered. Next, using the Si filter has drastically cut down the power to 90%, yet still showing response.

Further, it is shown that as the applied voltage increases the collection efficiency, the response current also increases, as seen in figure 6b.

Measurement of the optical reflectance and further calculation of QE, IQE, and responsivity were carried out using equations 1 and 2 for a MSM detector made up of a $\text{Si}_{0.85}\text{Ge}_{0.15}/\text{Si}$, which was wet-etched for 10 min, as indicated earlier. The reflectance, QE (λ), and spectral responsivity of a 15% Ge-containing $\text{Si}_{0.85}\text{Ge}_{0.15}/\text{Si}$, which was wet-etched for 10 min prior to the fabrication of the MSM detector, are plotted with respect to the wavelength and shown in figure 7. The measurements were taken without any applied voltage at zero bias.

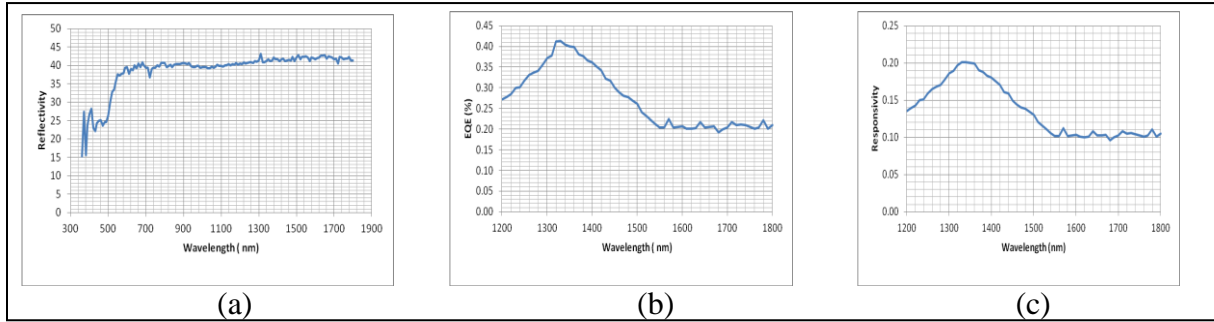


Figure 7. (a) Reflectance of the sample $\text{Si}_{0.85}\text{Ge}_{0.15}/\text{Si}$ etched for 10 min, (b) QE (λ), and (c) spectral responsivity of the same sample with zero bias.

These results obtained in our experiments are similar to or even better than some of the other work for a zero bias applied voltage (20).

4. Conclusion

We fabricated MSM detectors using wet-etched SiGe/Si samples with varying amounts of Ge, and studied their electrical properties of I-V, optical response, QE, and responsivity under zero bias and the results reported. We observed increased response current as the amount of Ge increased in the sample. Similarly, we observed enhanced response current as we changed the etching time of the sample indicative of increased absorption. The significance of this work is that for the first time, infrared detection beyond the band edges of both silicon and gallium arsenide is shown to be feasible with black-SiGe. Although the response is low, this is due, for the most part, to the small initial thickness of the SiGe layer. Because the absorption coefficients of Si, Ge, and SiGe are much smaller than that of, say, InGaAs, much larger thicknesses are required to obtain the same absorbance. The SiGe layers of this work are less than one micron; so clearly, for future work, thicker layers will provide dramatically better response than that shown here. However, the key point from this work is that there is a clear path toward very-low cost infrared sensing technology that employs blackened SiGe.

5. References

1. Younkin, R.; Carey, J.; Mazur, E.; Levinson, J.; Friend, C. *J. Appl. Phys.* **2003**, 93 (5), 2626.
2. Crouch, C.; Carey, J.; Shen, M.; Mazur, E.; Genin, F. *Appl. Phys A* **2004**, 79, 1635.
3. Huang, Z.; Carey, J.; Liu, M.; Guo, X.; Mazur, E.; Campbell, J. *Appl. Phys. Lett.* **2006**, 89, 033506.
4. Konig, U.; Gruhle, A. *Proceedings of the 1997 IEEE/Cornell Conference on Advanced Concepts in High Speed Semiconductor Devices and Circuits*, IEEE, Ithaca, NY, 1997.
5. Grimmeiss, H. G. *Semiconductors* **1999**, 33, 939.
6. Nayak, D. K.; Woo, J. C.; Park, J. S.; Wang, K. L.; MacWilliams, K. P. *IEEE Electron Device Lett. EDL-12-154* **1991**.
7. Luryi, S.; Kastalsky, A.; Bean, J. C. *IEEE Trans. Electron Devices ED-31* **1984**, 1135.
8. Perasall, T. P.; Bean, J. C. *IEEE Electron Device Lett. EDL-7* **1986**, 308.
9. Venkataraman, V.; Liu, C. W.; Strum, J. C. *J. Vac. Sci. Technol* **1993**, B 11, 1176.
10. Williamson, D. L. *Solar Energy Materials and Solar Cells* **2003**, 78 (1–4), 41–84.
11. Chueh, Y. L.; Fan, Z.; Takei, K.; Ko, H.; Kapadia, R.; Rathore, A. A.; Miller, N.; Yu, K.; Wu, M.; Haller, E. E.; Javey, A. *Nano Lett.* **2010**, 10, 520.
12. Koynov, S.; Brandt, M. S.; Stutzmann, M. *App. Phys. Lett.* **2006**, 88, 203107.
13. Wu, C.; Crouch, C. H.; Zhao, L.; Carey, J. E.; Yonkin, R.; Levinson, J. A.; Mazur, E.; Farrell, R. M.; Gothoskar, P.; Karger, A. *App. Phys. Lett.* **2001**, 73, 1850.
14. Nakajima, K.; Usami, N.; Fujiwara, K.; Murakami, Y.; Ujihara, T.; Sazaki, G.; Shishido, T. *Sol. Energy Mater. Sol. Cells* **2002**, 72, 93.
15. Nakajima, K.; Usami, N.; Fujiwara, K.; Murakami, Y.; Ujihara, T.; Sazaki, G.; Shishido, T. *Sol. Energy Mater. Sol. Cells* **2002**, 73, 305.
16. Kasper, E.; Presting, H. *SPIE* **1990**, 1361, 302.
17. Presting, H. *Thin Solid Films* 1998, 81, 1687.
18. People, R. *IEEE, J. Quantum Electr* 1086, QE-22:1696.

19. Semendy, F.; Taylor, P.; Meissner, G.; Wijewarnasuriya, P. *Black SiGe for Extended Wavelength Near Infrared Electro-Optical Applications*; ARL-TR-5202; U.S. Army Research Laboratory: Adelphi, MD, 2010.
20. Sorianello, V.; De Iacovo, A.; Colace, L.; Fabbri, A.; Torlora, L; Buffagni, E. *App. Phys. Lett.* **2012**, *101*, 081101.

NO. OF COPIES	ORGANIZATION	NO. OF COPIES	ORGANIZATION
1	ADMNSTR DEFNS TECHL INFO CTR ATTN DTIC OCP 8725 JOHN J KINGMAN RD STE 0944 FT BELVOIR VA 22060-6218	1	US GOVERNMENT PRINT OFF DEPOSITORY RECEIVING SECTION ATTN MAIL STOP IDAD J TATE 732 NORTH CAPITOL ST NW WASHINGTON DC 20402
1	DARPA MTO ATTN N DHAR 3701 NORTH FAIRFAX DR ARLINGTON VA 22203-1714	1	DIRECTORATE FOR ENGRG ECCS DIV NATIONAL SCIENCE FOUNDATION ATTN A B KAUL 4201 WILSON BLVD, RM 525 ARLINGTON VA 22230
1	US ARMY RSRCH DEV AND ENGRG CMND ARMAMENT RSRCH DEV & ENGRG CTR ARMAMENT ENGRG & TECHNLOGY CTR ATTN AMSRD AAR AEF T J MATTS BLDG 305 ABERDEEN PROVING GROUND MD 21005-5001	1	GENERAL TECHNICAL SERVICES ATTN G P MEISSNER 3100 ROUTE 138 WALL NJ 07719
1	ARMY RESEARCH OFFICE ATTN RDRL ROE L W CLARK III PO BOX 12211 RESEARCH TTRIANGLE PARK NC 27709	62	U.S. ARMY RSRCH LAB ATTN RDRL SEE I S TRIVEDI ATTN IMAL HRA MAIL & RECORDS MGMT ATTN RDRL CI J PELLEGRINO ATTN RDRL CIO LL TECHL LIB ATTN RDRL CIO LT TECHL PUB ATTN RDRL SE T BOWER ATTN RDRL SEDE E B MORGAN ATTN RDRL SEDE E K A JONES ATTN RDRL SEDE E M LITZ ATTN RDRL SED P A LELIS ATTN RDRL SEE E N GUPTA ATTN RDRL SEE E R TOBER ATTN RDRL SEE E W CHANG ATTN RDRL SEE G WOOD ATTN RDRL SEE I B ZANDI ATTN RDRL SEE I D BEEKMAN ATTN RDRL SEE I F SEMENDY (12 COPIES) ATTN RDRL SEE I G BRILL ATTN RDRL SEE I J LITTLE ATTN RDRL SEE I K K CHOI ATTN RDRL SEE I K OLVER ATTN RDRL SEE I K S RAMSEY ATTN RDRL SEE I P FOLKES ATTN RDRL SEE I P TAYLOR ATTN RDRL SEE I P UPPAL ATTN RDRL SEE I S SVENSSON ATTN RDRL SEE I W BECK
2	CECOM NVESD ATTN AMSEL RD NV A SCHOLTZ ATTN AMSEL RD NV D BENSON 10221 BURBECK RD STE 430 FT BELVOIR VA 22060-5806		
1	CM ACOUSTIC AND NETWORKED SENSORS DIV ATTN V SWAMINATHAN PICATINNY NJ 07806-5000		
1	US ARMY ARDEC-BENET LABS ATTN J WARRENDER WATERVLIET ARSENAL NY 12189		
1	US ARMY INFO SYS ENGRG CMND ATTN AMSEL IE TD A RIVERA FT HUACHUCA AZ 85613-5300		

NO. OF
COPIES

ORGANIZATION

ATTN RDRL SEE I W SARNEY
ATTN RDRL SEE I Y CHEN
ATTN RDRL SEE L BLISS
ATTN RDRL SEE M G DANG
ATTN RDRL SEE M G GARRETT
ATTN RDRL SEE M M REED
ATTN RDRL SEE M
M TAYSING-LARA
ATTN RDRL SEE M
M WRABACK
ATTN RDRL SEE M N BAMBHA
ATTN RDRL SEE M N DAS
ATTN RDRL SEE M P SHEN
ATTN RDRL SEE O N FELL
ATTN RDRL SEE O
P PELLEGRINO
ATTN RDRL SEE P GILLESPIE
ATTN RDRL SEG N MARK
ATTN RDRL SER E A DARWISH
ATTN RDRL SER E P SHAH
ATTN RDRL SER L
A WICKENDEN
ATTN RDRL SER L B NICHOLS
ATTN RDRL SER L E ZAKAR
ATTN RDRL SER L M DUBEY
ATTN RDRL SER L M ERVIN
ATTN RDRL SER L
S KILPATRICK
ATTN RDRL SER
P AMIRTHARAJ
ADELPHI MD 20783-1197